

CENTRAL LASER FACILITY

Rutherford Appleton Laboratory

Annual Report 1995 - 96

Central Laser Facility
Rutherford Appleton Laboratory
Chilton, Didcot
Oxfordshire OX11 0QX
Tel. (0)1235 - 445582
Fax. (0)1235 445888

RAL Report TR-96-066

The front cover shows the view through the Titania laser cell into the multiplexing area.

The back cover shows part of the Titania pulsed power area in R2.

ISBN 0902376454

INTERACTION OF A SHORT, INTENSE LASER PULSE WITH A PREFORMED PLASMA

M. Borghesi, L. Barringer, L.A. Gizzi*, A.J. MacKinnon, C. Meyer and O. Willi

The Blackett Laboratory, Imperial College of Science, Technology and Medicine, London

* TESRE-CNR, Bologna (Italy)

INTRODUCTION

The propagation of an intense laser pulse through a plasma is a fundamental requirement for a number of applications [1] such as particle acceleration via plasma waves, x-ray laser studies [2], and the Fast Ignitor scheme for ICF [3]. In particular, the Fast Ignitor scheme requires the short laser pulse not only to propagate without considerable energy loss through the underdense coronal plasma, but also to penetrate into the overdense region of the imploding plasma. For a sufficiently powerful, long laser pulse, self guiding of the pulse due to relativistic effects is predicted by theory [4]. Indirect experimental observations of this phenomenon have been reported, in which relativistic channelling of a short pulse in a tenuous plasma was diagnosed via Thomson scattering [5]. A relativistic effect also predicted [6] but not yet experimentally observed, is overdense penetration of a laser pulse at relativistic intensity, due to relativistic increase of the mass of the electrons.

An experimental study of the propagation of a picosecond laser pulse at relativistic intensities through preformed plasmas is presented here.

EXPERIMENTAL ARRANGEMENT

The experiment was performed at the Central Laser facility using the Vulcan laser in the CPA operation mode. The targets used were plastic foils. Their thicknesses varied in the range 0.1-0.5 μm . The plasma was preformed by a 400 ps pulse, frequency doubled in a KDP crystal to $\lambda = 0.527 \mu\text{m}$ and focused onto target in a spot of around 200 - 300 μm in diameter, at irradiances below 10^{13} W/cm^2 . Different oscillators (YLF, LML, Ti:Sa) were used throughout the experiment to generate the 1.054 μm interaction pulse. Typical operating parameters for the interaction pulse were 10-20 J on target in a pulse duration of 1-4 ps, focused in a spot of 10-20 μm in diameter. Consequently, intensities above 10^{18} W/cm^2 were obtained on an average shot.

Both heating and interaction beams were focused onto target by an f/5 Off-Axis Parabolic mirror (OAP). The green heating beam was injected into the short pulse beamline through the back of the last turning mirror before the OAP. A small divergence was

imposed on the heating beam with a telescope, in order to obtain a heating focal spot much larger than the one of the interaction beam. The delay between heating and interaction pulses could be varied, thus allowing interaction with the plasma at different stages of its evolution.

The plasma was diagnosed with a temporally independent probe pulse, which was split-off of the uncompressed interaction beam. The probe pulse was then compressed on a pair of gratings and frequency doubled in a KDP crystal, resulting in a probe wavelength of 0.527 μm and a pulse duration of few picoseconds. The spatial resolution of the optical system was about 1 μm . A Nomarsky modified interferometer [7] allowed 2-D, time resolved density maps of the preformed plasma to be obtained. Schlieren photography [8] with a sensitivity of 5 mrad, was used to observe the effects of the interaction on the plasma. Polarimetry [8] measurements were also performed in order to detect magnetic fields generated during the interaction. These last measurements, very sensitive to emission noise, required the probe wavelength to be Raman shifted to 622 nm. An f/2.5 lens collected the radiation transmitted through the plasma. Two Streak Cameras, set respectively to collect green and infrared light, were used to observe, with resolution of few picoseconds, the temporal evolution of the transmitted radiation. Spectra of the backscattered radiation were obtained with grating spectrometers using a 1200 lines/mm grating (linear dispersion 15 $\text{\AA}/\text{mm}$).

EXPERIMENTAL RESULTS

Initially, the preformed plasma was characterised via interferometry. In fig.1, an interferogram taken 130 ps after the peak of the heating beam is shown, together with the density map obtained from it. The heating irradiance was $5 \times 10^{12} \text{ W/cm}^2$, in a focal spot of about 300 μm in diameter (FWHM). As it can be seen from the reconstructed density profile, density measurements were possible only for electron density values lower than 10^{20} cm^{-3} . In fact, in the high density region closer to the original target position, the density gradients were large enough to refract the probe light out of the collecting optics. The density profile in these regions was inferred by 1-D simulations, performed with the hydrocode MEDUSA.

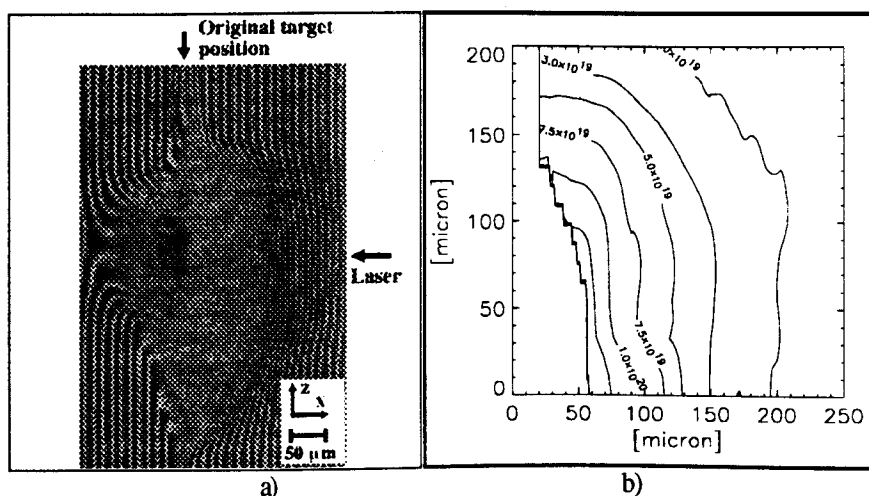


Fig. 1. a) Interferogram of the preformed plasma, taken 100 ps after the peak of the heating beam (0.527 μm , 400 ps), for an heating beam irradiance of $5 \times 10^{12} \text{ W/cm}^2$. b) 2-D electron density map obtained from the interferogram.

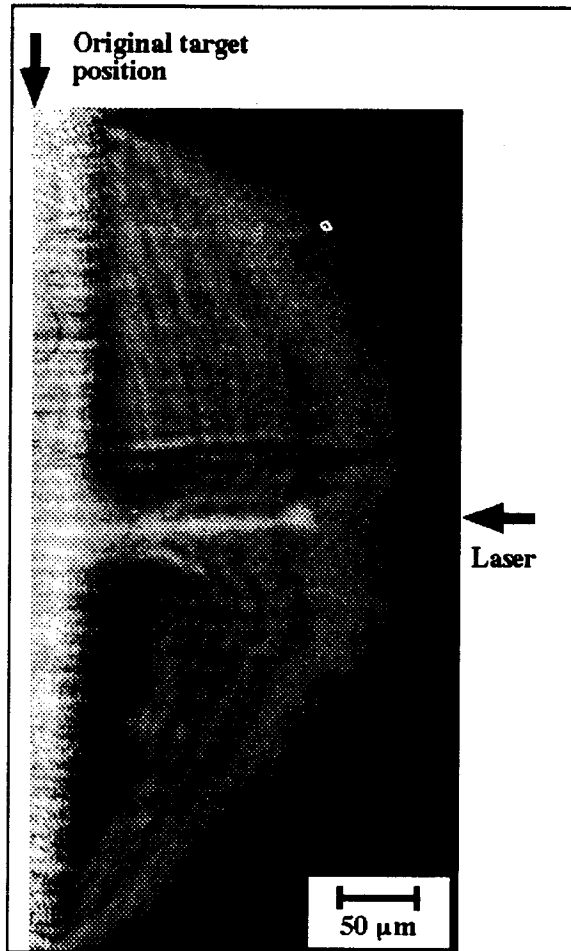


Fig. 2. Time-resolved Schlieren image taken 30 ps after the interaction of an 1 ps, 1.054 μm pulse at irradiance $3.5 \times 10^{18} \text{ W/cm}^2$ with the preformed plasma of Fig. 1. The narrow channel feature visible in the centre of the plasma is due to time integrated second harmonic emission.

INTERACTION WITH UNDERDENSE PLASMAS

The optical probe was also used to diagnose the interaction. In Fig. 2, a Schlieren image of the plasma is shown, taken 30 ps after the interaction with the preformed plasma of Fig. 1. The power of the interaction pulse was 10^{13} W . The focal spot was 20 μm in diameter, giving an average irradiance of $3.2 \times 10^{18} \text{ W/cm}^2$. The density distribution 30 ps after the interaction is imaged, with picosecond temporal resolution.

The most striking feature in the image is the narrow second harmonic emission filament visible in the centre of the plasma. This feature, present in a high number of experimental observations, is time-integrated, and corresponds to radiation emitted during the interaction. It can therefore be interpreted as a signature of the spatial extent of the interaction beam in the plasma. The diameter of the channel is about 5 μm, while its length is about 130 μm, i.e. more than 6 times the Rayleigh length corresponding to the diameter size. From comparison with the preformed plasma profile, it can be seen that the laser pulse focuses down to a 5 μm size at a density of $0.05 n_c$. It has to be noted that the laser power was well above the threshold for relativistic self-focusing [4] at that density.

Strong channelling of the pulse in near critical underdense plasma was recently predicted by 3-D PIC simulations [9] (fig. 3). The physical mechanisms involved in the channelling process are the

following: as the short pulse undergoes relativistic self-focusing, fast electrons are accelerated in the direction of laser propagation, generating large quasi-static magnetic fields. The magnetic fields are in turn effective in pinching the electron current, confining it into a narrow, collimated beam. The propagating laser light follows the electron deflection and, consequently, the pulse channels itself through the plasma.

The results obtained with the other diagnostics seem to confirm the scenario described above. Second harmonic spectra of the backscattered radiation showed a pronounced red shifted broadening, that can be explained as a Self Phase Modulation (SPM) effect in the context of the channelling assumption. As the pulse self-focuses into the channel, ponderomotive expulsion of the electrons, and consequently of the ions, takes place. The pulse then travels through a medium in which the refractive index is rapidly varying, and consequently the phase of the pulse is modulated. Since the derivative of the refractive index stays positive during the pulse propagation, the broadening is on the red side of the spectrum [10]. Two scenarios are plausible: either the interaction pulse undergoes SPM during the propagation (and then transfers the modulation to the second harmonic radiation emitted) or the 2ω itself is directly phase modulated. For the interaction conditions of fig. 3 typical broadening observed were in the range 400 - 600 Angstrom.



Fig. 3. Polarigram taken during the short pulse interaction with a preformed plasma in the same conditions of fig. 1.

Preliminary measurements of the magnetic fields generated during the interaction were also performed, with a polarimetric technique (for details on the experimental method see M. Borghesi et al., *Measurements of self-generated*, also in this report). From the polarigram the rotation undergone by different parts of the probe beam, and consequently the magnetic field distribution, can be reconstructed. From the polarigram of fig. 4, taken during the interaction, the presence of two different type of toroidal magnetic fields is suggested. The first (with an amplitude of a fraction of a MG), corresponds to the rotation detectable on the outer edge of the plasma, on the laser side. The second, more intense field (about 2 MG), correspond to the bright and dark regions closely surrounding the laser axis. The direction of the field on the outer edge of the plasma is as expected in case of field generation due to $\nabla n \times \nabla T$ mechanisms [11]. No field was measured in absence of interaction, so the density and intensity gradients generating the fields are produced (or considerably enhanced) by the interaction pulse. Direction and amplitude of the inner field would substantially agree with the PIC code predictions for the quasi-static magnetic fields responsible for pinching the

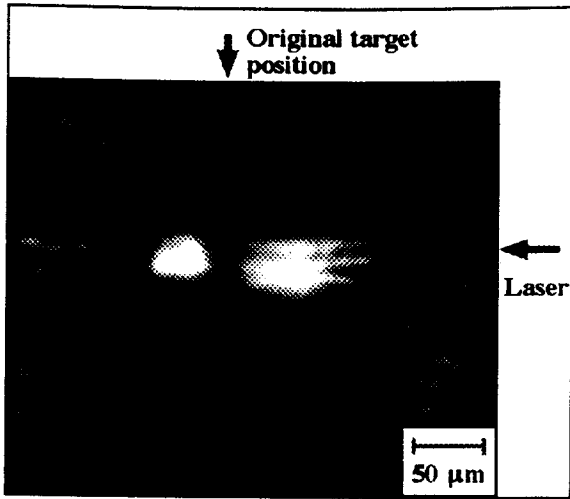


Fig. 4. Time-resolved Schlieren image taken 30 ps after the performed plasma in conditions close to Fig.2. Three second harmonic emission channels, that coalesce in a single structure, are visible in the picture.

short pulse and confining it into the channel. Further investigations are however necessary to confirm these assumptions.

In some experimental observations, the laser beam appeared to break up into more than one filament, and coalescence of the corresponding emission channels in a single structure was observed. In the Schlieren image of fig. 4, three filamentary structures are visible, that collapse in a single channel as they propagate through the plasma. Such phenomenon was also observed in 2-D and 3-D [9] PIC simulations, and was attributed to magnetic interaction between the filaments.

INTERACTION WITH OVERDENSE PLASMAS

The interaction with an overdense plasma was also studied. In particular, an experimental method for the detection of overdense propagation was devised and tested. In fig. 5 experimental results obtained with the Streak Camera set to collect the green transmitted radiation are shown. It can be seen that the target is transparent to the rising edge of the heating pulse, before a

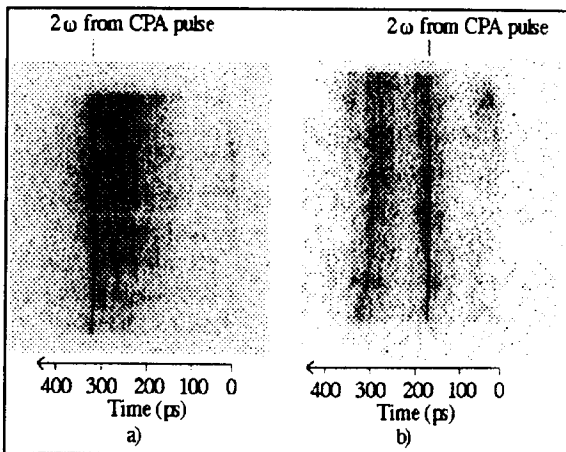


Fig. 5. Temporal evolution of the green radiation transmitted through the plasma, for an heating beam irradiance of 7×10^{12} W/cm². In a) the delay between the CPA pulse and the heating beam was 320 ps, and the CPA irradiance 2×10^{18} W/cm². In b) the delay was 165 ps and the CPA irradiance 3.5×10^{18} W/cm².

plasma is created. Then, as soon as an initially overdense plasma is created, no heating radiation is transmitted, until the plasma goes underdense. A sharp line is also visible, due to 2ω emission generated by the interaction pulse. This feature can be considered as a time fiducial of the interaction, and used to infer, from comparison with 1-D simulation and interferometric data, at which stage of the plasma evolution the interaction took place. For the situation of fig. 5b, the MEDUSA predictions suggest that the pulse propagated through a plasma of peak density 2×10^{21} cm⁻³ ($2n_c$ for $\lambda=1 \mu\text{m}$). The theory [6] predicts an increase of the effective critical density seen by the pulse given by

$$n_{c,eff} = n_{c0} \left(1 + \frac{I\lambda^2}{10^{18}}\right)^{0.5}$$

An intensity of 3×10^{18} W/cm² is therefore just sufficient to propagate through a plasma of density $2n_c$. Due to the limited number of data available, this has to be considered more a study of feasibility than a conclusive experimental study.

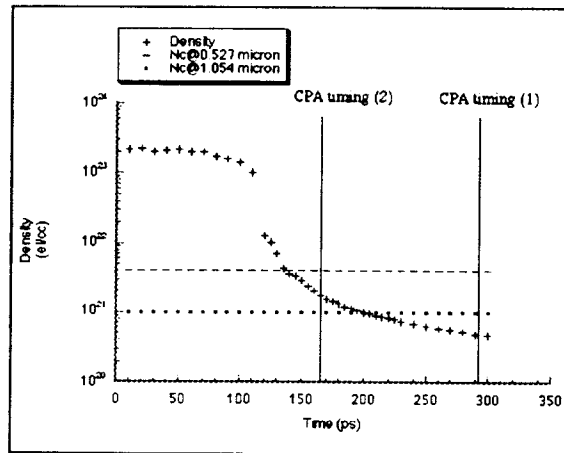


Fig. 6. Plasma peak density vs time as predicted by 1-D simulations (MEDUSA 102) for the heating conditions of fig. 5. The vertical lines show the CPA timing in the shots of fig. 5.

CONCLUSION

The interaction of short pulses at relativistic intensities with preformed plasmas has been experimentally studied in different plasma conditions. The propagation in near critical underdense plasmas appeared to be characterised by strong self channelling of the pulse, as predicted by 3D PIC simulations. A preliminary study of the possibility of overdense propagation has also been performed.

REFERENCES

1. W.Tajima and J.Dawson, Phys.Rev.Lett. **43**, 267 (1979)
2. D.C.Eder, P.Amendt, S.C.Wilks, Phys.Rev.A **45**, 6761 (1992)
3. M.Tabak et al, Phys. Plasmas **1**, 1626 (1994)
4. P.Sprangle, E.Esarey, Phys.Fluids B **4**, 2241 (1992)
5. P.Monot et al., Phys.Rev.Lett. **74**, 2953 (1995)
6. P.Kaw, J.Dawson, Phys. Fluids **13**, 472 (1970)
7. R.Benattar, C.Popovics, R.Sigel, Rev. Sci. Instruments **50**, 1583 (1979)
8. O.Willi, in *Laser Plasma Interaction 4*, Proceedings of the XXXV SUSSP, St Andrews (1988)
9. A.Pukhov and J.Meyer ter Vehn, Phys. Rev. Lett. to be published (1996)
10. D.Giulietti et al, Opt. Comm. **106**, 52 (1994)
11. J.A.Stamper, Laser & Part. Beams, **9**, 841 (1991)